# Development of Frictional Pressure Drop Correlation for Single- and Two-phase Flow in Helically Coiled Tube

Oktari Zaidi, Byong Jo Yun, Jae Jun Jeong\*
School of Mechanical Engineering, Pusan National University (PNU)
\*Corresponding author: jjjeong@pusan.ac.kr

\*Keywords: helically coiled tube, single-phase, two-phase, frictional pressure drop.

#### 1. Introduction

Helically coiled tubes (HCTs) are widely used in steam generators of small modular reactors (SMRs) for their compact design and heat transfer performance [1]. However, the curved geometry forces a continuous change in flow direction, inducing centrifugal force that generates secondary flow that rotates perpendicular to the primary flow. This motion creates a more tortuous path, significantly increasing the frictional pressure drop by elevating the overall flow resistance [2]. Accurate prediction of this pressure drop is essential for reliable design and safe operation of SMRs.

Flow in HCTs is governed by the combined influence of centrifugal force, gravity, and secondary flows, which makes predicting frictional pressure drop more challenging. In single-phase flow, most existing correlations rely on Reynold number (Re) and curvature ratio (d/D) as the key parameters, but their accuracy is often limited to narrow ranges of geometry and flow conditions. Moreover, these parameters do not explicitly capture and quantify the contribution of centrifugal force to the pressure drop.

In two-phase flow, centrifugal force drives phase separation, concentrating liquid toward the outer wall and vapor on the inner wall. This causes non-uniform phase distribution and changes in flow structure, which affect the pressure drop. Although numerous correlations have been proposed, they are often derived from limited operating conditions, so their accuracy further decreases when applied outside those range and neglect the influence of centrifugal force.

This study focuses on developing new correlations for predicting single- and two-phase frictional pressure drops in helically coiled tubes. Large experimental databases were collected and analyzed to identify key parameters, with special attention to the role of centrifugal force. Using this data, new models were formulated and assessed against best-performing existing correlations.

### 2. Experimental Database

# 2.1 Single-phase flow database

The database was built from 13 published studies using water as the working fluid in smooth vertical HCTs.

To distinguish the flow regimes of laminar and turbulent, the critical Reynold number based on the Schmidt correlation [3], was used to identify fully developed turbulent flow regime. The final dataset contains 1,489 data points. A summary of the resources and parameter ranges is given in Table 1.

Table 1. Experimental database for single-phase flow.

Goometry				101 51	Data points*)		
Authors		Geometry		Re		its*)	
Authors	d (mm)	d/D	P <sub>c</sub> (mm)	$(x10^3)$	L	Т	Total
Akagawa et al. [4]	9.92	0.044- 0.09	14.86- 14.91	0.25- 18	83	28	111
Ali et al. [5]	4.64- 6.03	0.026- 0.052	10-50	0.3- 17	102	43	145
Austen et al. [6]	4.57	0.02	23- 265	0.08- 5	22	0	22
Awwad et al. [7]	25.4	0.073	194	1- 62	5	15	20
Cioncolini et al. [8]	4.04- 10.44	0.003- 0.144	7-25	1- 63	412	350	762
Colombo et al. [9]	12.53	0.012	800	1.8- 29	23	41	64
Ju et al. [10]	18	0.16	22.5	3- 11	7	0	7
Liu et al. [11]	4.4	0.021- 0.066	4.4- 13.2	0.16- 10	91	8	99
Rogers et al. [2]	7.4-9.5	0.05- 0.093	38.1- 102	3- 48	20	39	59
Seban et al. [12]	7.4	0.059	102	8- 61	0	48	48
Guo et al. [13]	10	0.076	39	43- 150	0	24	24
Zheng et al. [14]	14	0.013- 0.035	110- 582	5-120	0	66	66
Hardik et al. [15]	5.4- 7.5	0.036- 0.05	50	7- 17.5	0	62	62
All	4.4- 25.4	0.003- 0.16	7- 800	0.08- 150	765	724	1489

<sup>\*)</sup> L= laminar, T=Turbulent.

## 2.2 Two-phase flow database

Two-phase steam-water frictional pressure drop data for HCTs were collected from the dataset of Santini et al. [16], Xiao et al. [17], Zheng et al. [14], and Su et al. [18]. The data covers a wide range of geometry and operating conditions. The assembled data contains 876 data points, as summarized in Table 2.

Table 2. Experimental database for two-phase flow.

	Geometry			Operating parameters			Data
Authors	d (mm)	d/D	P <sub>c</sub> (mm)	P (MPa)	G (kg/m <sup>2</sup> s)	x	points
Santini et al. [16]	12.53	0.0125	800	2-6	200-800	0.1- 0.99	643
Xiao et al. [17]	12.5- 14.5	0.033- 0.08	59.44- 125.5	2-8	300-1100	0.06- 0.7	104
Zheng et al. [14]	14	0.008- 0.035	110- 582	2-7.6	100-1200	0.12- 0.91	57
Su et al.[18]	12	0.107	22.5	3.5-7	320-1100	0.1- 0.9	72
All	12.5- 14.5	0.008- 0.107	22.5- 800	2-8	100-1200	0.06- 0.99	876

#### 3. Development of a new correlation

# 3.1 A new friction factor correlation for single-phase flow

The friction factor data in HCTs were analyzed with respect to Reynold numbers and curvature. Fig. 1 shows the measured coil friction factor,  $f_c$  divided by straight tube friction factor,  $f_s$  versus Reynold number and curvature. As can be seen,  $f_c/f_s$  exhibits clear dependence on both parameters which consistent with a trend observed in previous studies [4,6]. To capture and quantify the effect of centrifugal force in single-phase frictional pressure drop, the centrifugal force number  $(N_{CF})$  proposed by Jeong et al. [19] is adopted, which is defined as:

$$N_{CF} = \frac{\rho v_{\theta}^{2} / (D/2)}{\rho g} \tag{1}$$

where  $v_{\theta}$  is the horizontal (azimuthal) component of the fluid velocity, and defined as:

$$v_{\theta} = \frac{1}{\sqrt{1 + \left(P_c/\pi D\right)^2}} v \tag{2}$$

By substituting Eq. (2) to (1), the centrifugal force number in single-phase flow will become:

$$N_{CF} = 2\frac{v^2}{gD} \frac{1}{1 + (P_c/\pi D)^2} = 2Fr \frac{d}{D} \frac{1}{1 + (P_c/\pi D)^2}$$
 (3)

where Fr is the Froude number  $(v^2 / gd)$ .

The result in Fig. 2 show  $f_c/f_s$  increases with  $N_{CF}$  in both regimes. In laminar flow, the rise is steep because the stable velocity profile allows centrifugal force to redistribute momentum toward the outer wall and increase average flow resistance and pressure drop [12]. In turbulent flow,  $f_c/f_s$  also increases but more gradually, because turbulence already promotes intense mixing and momentum exchange through chaotic vortical structures, which reduce the relative effect of centrifugal force. Even though  $N_{CF}$  range is broader in turbulent flow due to stronger inertia, the relative increase in wall friction induced by centrifugal force remains smaller than in laminar flow [4]. These results show that  $N_{CF}$ , together

with *Re* and curvature, govern frictional pressure drop in HCTs

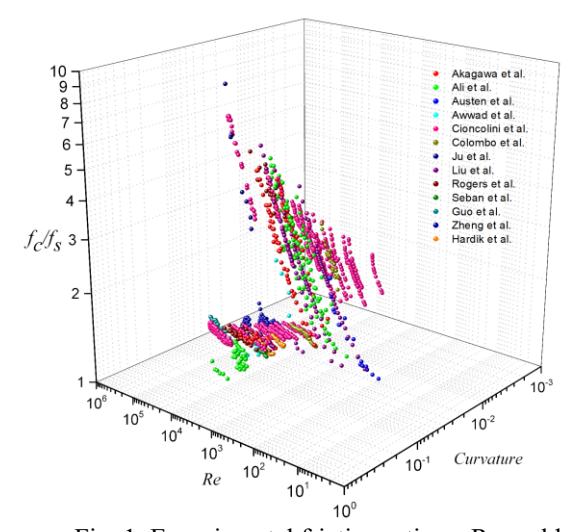
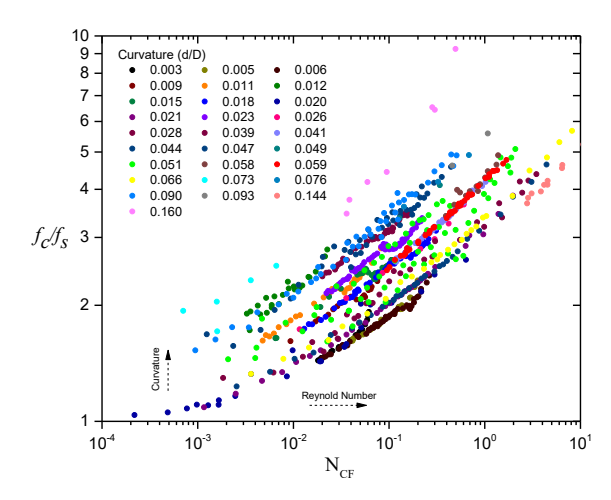


Fig. 1. Experimental friction ratio vs Reynold number and curvature.



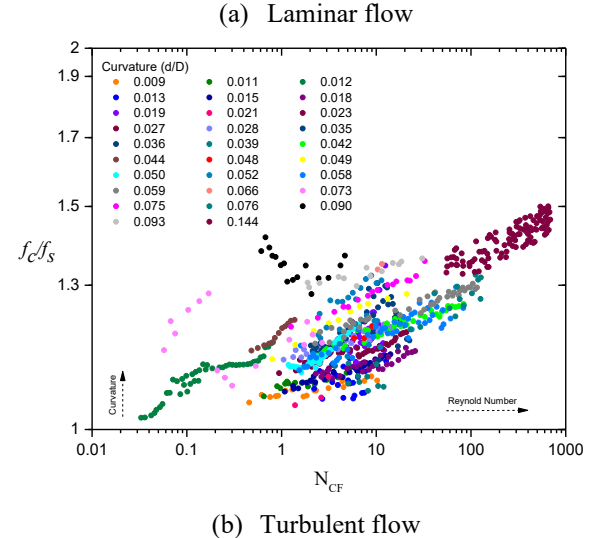


Fig. 2. Friction factor vs  $N_{CF}$  in single-phase flow.

Pearson correlation coefficient [21] then used to statistically quantify the relationship between  $f_c/f_s$ , Re, curvature (d/D), and  $N_{CF}$  for laminar and turbulent flows, using the data ranges listed in Table 3. The heatmaps Fig. 3 show d/D has the strongest correlation, followed by  $N_{CF}$  and Re. Because  $N_{CF}$  is strongly correlated with d/D, multicollinearity was checked using variance inflation factor (VIF). As shown in Table 4, all VIF values are below 5 which is the threshold values [22], confirming the parameters can be used together in the model.

Table 3. The range of non-dimensional parameters used for modeling in single-phase flow.

for medering in single phase new.					
Parameter	Laminar	Turbulent			
f <sub>c</sub> /f <sub>s</sub>	1.03 - 9.25	1.022 - 1.5			
Re	84.82 – 11642.06	5849.63 – 149500.5			
d/D	0.003 - 0.16	0.0096 - 1.05			
$N_{CF}$	0.0002 - 47.88	0.04 - 687.1			

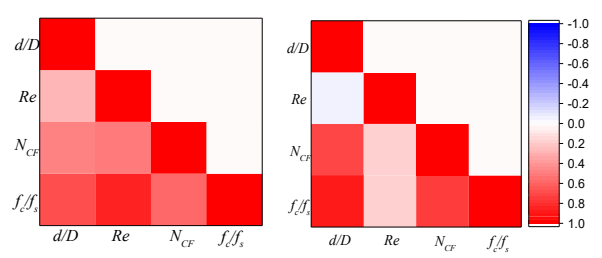


Fig. 3. Pearson correlation coefficients heatmaps for laminar (left) and turbulent (right) flow regimes.

Table 4. VIF measurement for single-phase.

D .	Lan	inar	Turbulent		
Parameter	$R_i^2$	$VIF_i$	$R_i^2$	$VIF_i$	
d/D	0.24	1.31	0.58	2.38	
Re	0.26	1.36	0.12	1.14	
$N_{CF}$	0.39	1.64	0.58	2.45	

Using the selected parameters mentioned in previous section and nonlinear least squares method fitting process within the applicability range summarized in Table 3, empirical correlations were formulated for laminar and turbulent regimes as follows.

For laminar flow:

$$\frac{f_c}{f_s} = 1 + 0.05Re^{0.591} (d/D)^{0.34} N_{CF}^{0.018}$$
 (4)

For turbulent flow:  

$$\frac{f_c}{f_s} = 1 + 0.143 Re^{0.189} (d/D)^{0.526} N_{CF}^{0.027}$$
(5)

Both correlations converge to the straight tube behavior when the coil diameter approaches infinite. Under these conditions, the correlations simplify the original Blasius equation [23],  $f_s = 64/Re$  and  $f_s = 0.316Re^{-0.25}$  for laminar and turbulent respectively.

# 3.2 A new two-phase flow frictional pressure drop correlation

Two-phase flow frictional pressure drops often expressed using a dimensionless liquid-only two-phase multiplier which relates it to the corresponding singlephase flow frictional pressure drop:

$$\phi_{lo}^2 = \left(\frac{dP}{dz}\right)_{TP,fr} / \left(\frac{dP}{dz}\right)_{SP,lo} \tag{6}$$

In the homogeneous model (HM), where both phases move with equal velocity and temperature in constant cross-section, mixture density and viscosity from Mc Adams et al. [24] are used to evaluate the multiplier. In case of straight tube, the HM liquid-only multiplier will become Eq. (7) [25]. This expression serves as the baseline for developing the new two-phase frictional pressure drop correlation for HCTs in this study.

$$\phi_{lo,HM}^2 = \left[1 + x \left(\frac{\rho_l}{\rho_v} - 1\right)\right] \left[1 + x \left(\frac{\mu_l}{\mu_v} - 1\right)\right]^{-0.25}$$
(7)

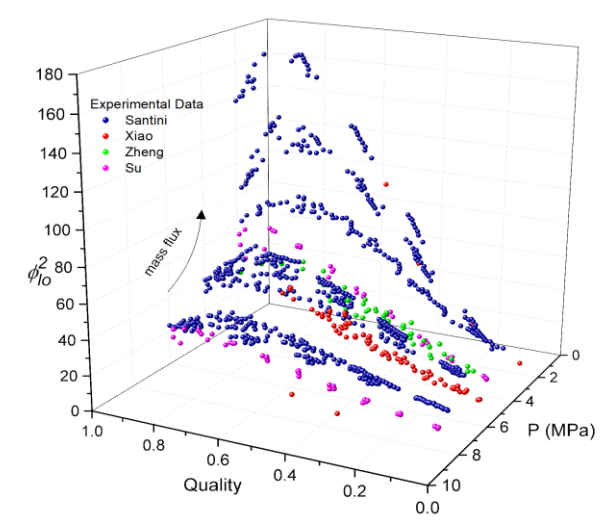


Fig. 4.  $\phi_{lo}^2$  vs pressure and quality.

The dominant parameters influencing the two-phase multiplier in HCTs were analyzed by plotting the experimental data using Eq. (6) at different pressures and quality, as shown in Fig. 4. Two-phase frictional pressure drops were obtained from the experimental database, while the corresponding single-phase pressure drop values were calculated using the new turbulent friction factor correlation in Eq. (5). The result shows that, at constant pressure, the multiplier increases with vapor quality, peaks near 0.8, then decreases as quality approaches unity. Meanwhile, at constant quality, higher system pressure decreases the multiplier by increasing vapor density, which raises mixture density and lowers mixture velocity. Conversely, higher mass flux increases the multiplier by intensifying secondary flows from centrifugal force which enhances phase interaction and leads to higher frictional pressure drop. The effect of centrifugal force is represented by reformulating  $N_{CF}$  into

liquid-only form, 
$$N_{CF,lo}$$
, given by:
$$N_{CF,lo} = 2Fr_{lo} \frac{d}{D} \frac{1}{1 + (P/\pi D)^2}$$
(8)

where 
$$Fr_{lo} = \frac{G^2}{gd\rho_m^2}$$
.

Since the model also expected to apply in both helical and straight tubes in HM model, a correction factor  $(\psi)$  is added to account the centrifugal force effects, and it expressed:

$$\phi_{lo}^2 = \psi \phi_{lo,HM}^2 \tag{9}$$

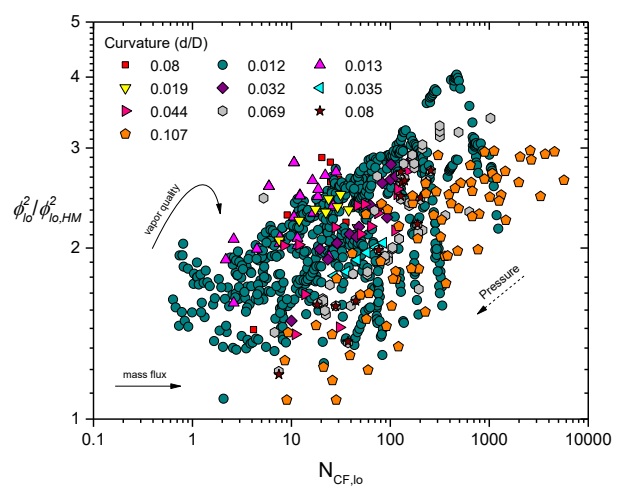


Fig. 5. Multiplier ratio vs  $N_{CF,lo}$  for different curvature ratios.

Centrifugal force dependence was then evaluated from multiplier ratio against  $N_{CF,lo}$  as shown in Fig. 5. The multiplier ratio does not form a single consistent trend with  $N_{CF,lo}$  because the  $N_{CF,lo}$  range varies with other parameters as indicated by the arrow sign. It shows that the multiplier ratio increases with increasing  $N_{CF,lo}$ , indicating that centrifugal force amplifies pressure drop in HCTs compared with straight tube. At low or moderate quality, a continuous film allows  $N_{CFIa}$  to enhance secondary flow and wall shear, raising the multiplier. While at high quality, the ratio decreases because the liquid film becomes thin and most liquid is carried in the vapor core, reducing wall friction [8] and decreases pressure drop despite a high  $N_{CF,lo}$ . The figure also indicates that as curvature increases, the multiplier ratio decreases because the value  $\phi_{lo}^2$  becomes smaller. This occurs since single-phase flow frictional pressure drop rises more rapidly with curvature than two-phase flow [1].

Subsequently, candidate parameters were examined using Pearson correlation coefficients as shown in Fig. 6, and VIF results in Table 5 were used to screen the influence of these parameters against correction factor,  $\psi$ , based on the data ranges summarized in Table 6. These show that  $\phi_{lo}^2$  and  $\phi_{lo,HM}^2$  are strongly correlated, confirming  $\phi_{lo,HM}^2$  as a reliable baseline.  $N_{CF,lo}$ ,  $Re_{lo}$ , and quality (x) show relatively high correlation with multiplier ratio. In addition, although not plotted in Fig. 6 or listed in Table 5, the density and viscosity ratios were also evaluated and found to have lower correlation and extremely high VIF values (>75) since their influence already included in the HM multiplier (Eq.(7)).

Curvature has the weakest negative correlation but a low VIF value, indicating no multicollinearity issue, and is retained to ensure correct asymptotic behavior when it approaches zero. Based on these findings, the correction factor,  $\psi$  depends on  $N_{CF,lo}$ ,  $Re_{lo}$ , quality (x), and d/D. The pressure effect is instead captured in  $N_{CF,lo}$  through its dependence on mixture density, while mass flux is reflected in  $Re_{lo}$ .

Table 5. VIF measurement for two-phase flow.

Parameter	$R_i^2$	$VIF_i$
d/D	0.31	1.45
$Re_{lo}$	0.32	1.47
$N_{CF,lo}$	0.41	1.68
х	0.18	1.22

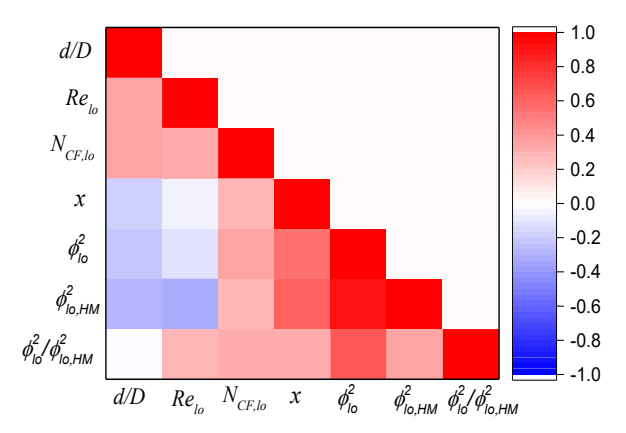


Fig. 6. Heatmap of Pearson's correlation for two-phase

Table 6. The range of non-dimensional parameters used for modelling in two-phase flow.

Parameter	Range of Data		
$\phi_{lo}^2/\phi_{lo,HM}^2$	1.08-4.04		
d/D	0.008-0.107		
$Re_{lo}$	20,048-144,736.8		
$N_{CF,lo}$	0.63-5,682		
х	0.06-0.99		

Following the previous steps, the correction factor model for two-phases was formulated as a function of the parameters within the range data presented in Table 6. After several iterations using non-linear least squares fitting, the obtained correction factor model is as follows:

fitting, the obtained correction factor model is as follows:  

$$\psi = \frac{1 + 0.012 N_{CF, lo}^{0.115} \left[ 1 + 22.62 x (1 - x)^{0.658} \right] Re_{lo}^{0.217}}{1 + 1.98 (d / D)^{0.796}}$$
(10)

The denominator represents the moderating role of the curvature ratio. This term limits the growth of the correction factor at high curvature, especially for Su et al. [18] dataset, where curvature is large and centrifugal force are dominant. It also ensures that the model approaches unity when curvature vanishes.

# 4. Assessment and comparison with best-existing correlations

#### 4.1 Assessment of single-phase correlation

Figure 7 illustrates the performance of the new model through predicted versus measured friction factor values. The results highlight that both laminar and turbulent predictions closely follow the reference line with narrow scatter. The data distribution remains tightly bounded within  $\pm 10\%$  error lines, showing significantly improved agreement.

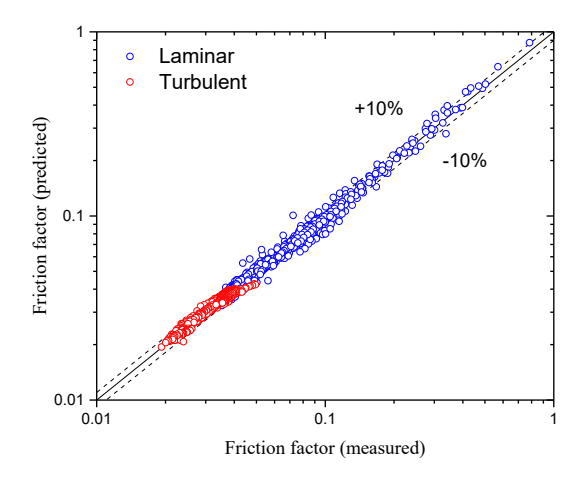


Fig. 7. Predicted vs measured friction factor coefficients for new model.

Table 7 further provides a detailed comparison of the predictive capability of both new and existing singlephase friction factor models. Among the existing correlations, Ito model [27] gives the most reliable performance across both laminar and turbulent regimes with low error and high accuracy within  $\pm 10\%$  error band. In contrast, Schmidt model [29] exhibits the poorest accuracy in laminar flow, while White model [26] shows the largest error in turbulent flow. Other models perform reasonably well but fall short compared to Ito. However, the new model which defined by Eqs. (4) and (5), outperform all existing models, achieving the lowest RMSE and the highest percentage data in both regimes also reducing RMSE by 7.0% in laminar and 9.1% in turbulent flow compared to Ito model which is the bestexisting models. This suggests that the new model provides a more accurate and reliable prediction of the friction factor across a broad range of flow conditions.

Table 7. Error comparison of new and existing friction factor models for single-phase flow.

Tuetor moue	81 <b>3</b> P1168	- 110		
Correlation	Laminar		Turbulent	
Correlation	RMSE	MRE	RMSE	MRE
White [26]	0.0701	0.0193	0.1882	-0.176
Ito [27]	0.0627	0.0057	0.0362	-0.001
Mori & Nakayama [28]	0.1915	0.0649	0.0383	0.002
Schmidt [29]	0.2858	0.2358	0.1302	-0.061
Mishra & Gupta [30]	0.0693	0.0193	0.0543	-0.039
New correlation	0.0583	0.0038	0.0329	-0.001

## 4.2 Assessment of two-phase correlation

Fig. 8 provides visual assessment of the new correlation against experimental measurements. The predicted values align closely with the measured frictional pressure gradients across the full data range. Furthermore, Table 8 compares statistical evaluation of new models against existing correlations. The result shows that classical correlations such as Lockhart-Martinelli [31], Ruffel [32], Friedel [33], and Zhao [34], show poor accuracy, while Colombo [9] performed the worst overall. Santini [35] and Ferraris [36] show better agreement with the data, while Su model [37] stands out as the best among existing models. Conversely, the new model achieves further improvements, reducing RMSE by 15% compared to Su and reaching the highest accuracy, with RMSE 0.1165 and 91.55% of data falling within error. Since the new correlation consistently outperforms all existing models across every dataset, all of which represent conditions closely to SMR operation, making it strongly recommended for the design and analysis of helical steam generators for SMRs.

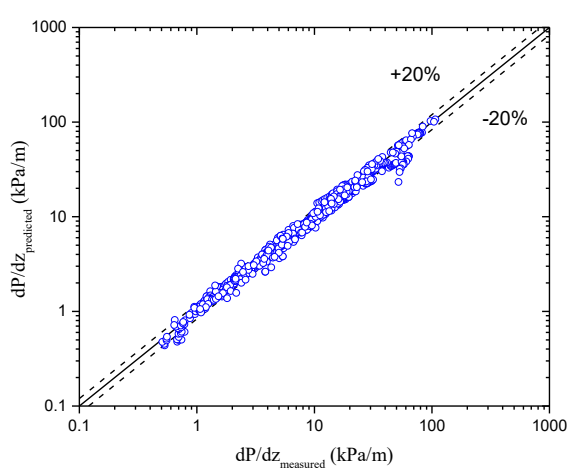


Fig. 8. Predicted vs measured two-phase frictional pressure drop for new model.

Table 8. Error comparison of new and existing friction factor models for two-phase flow.

Correlation	RMSE	MRE
Lockhart-Martinelli [31]	0.5060	-0.171
Ruffel [32]	0.3102	0.257
Friedel [33]	0.3971	0.350
Zhao [34]	0.4855	-0.426
Santini [35]	0.1852	0.105
Colombo [9]	0.8363	-0.659
Ferraris [36]	0.1519	0.045
Su [37]	0.1376	-0.008
New correlation	0.1165	0.012

#### 5. Conclusions

This study introduced new correlations for predicting frictional pressure drops in single- and two-phase flows through helically coiled tubes. The methodology combines key parameters analysis, statistical evaluation, and nonlinear regression. The findings show that in single- and two-phase flows, centrifugal force plays a major role in increasing frictional pressure drop. This effect was quantified through inclusion of the centrifugal force number in the correlation structure.

The correlations were developed using extensive experimental datasets and validated against the existing models. In both cases, the assessment results show that the new correlation achieves the highest accuracy, ensuring reliable applicability to the design and analysis of SMR steam generators.

#### REFERENCES

- [1] A. M. Fsadni and J. P. M. Whitty, "A review on the twophase pressure drop characteristics in helically coiled tubes," Applied Thermal Engineering, vol. 103, pp. 616–638, June 2016.
- [2] G. F. C. Rogers and Y. R. Mayhew, "Heat transfer and pressure loss in helically coiled tubes with turbulent flow," International Journal of Heat and Mass Transfer, vol. 7, no. 11, pp. 1207–1216, Nov. 1964.
- [3] E. F. Schmidt, "Wärmeübergang und Druckverlust in Rohrschlangen," Chemie Ingenieur Technik, vol. 39, no. 13, pp. 781–789, July 1967.
- [4] K. Akagawa, T. Sakaguchi, and M. UEDA, "Study On a Gas-Liquid Two-Phase Flow in Helically Coiled Tubes," Bulletin of JSME, vol. 14, no. 72, pp. 564–571, 1971.
- [5] S. Ali, "Pressure drop correlations for ow through regular helical coil tubes," Fluid Dyn. Res., vol. 28, pp 295-310, 2001. [6] D. S. Austen and H. M. Soliman, "Laminar flow and heat transfer in helically coiled tubes with substantial pitch," Experimental Thermal and Fluid Science, vol. 1, no. 2, pp. 183–194, Apr. 1988.
- [7] A. Awwad, R. C. Xin, Z. F. Dong, M. A. Ebadian, and H. M. Soliman, "Measurement and correlation of the pressure drop in air-water two-phase flow in horizontal helicoidal pipes," International Journal of Multiphase Flow, vol. 21, no. 4, pp. 607–619, 1995.
- [8] A. Cioncolini and L. Santini, "An experimental investigation regarding the laminar to turbulent flow transition in helically coiled pipes," Experimental Thermal and Fluid Science, vol. 30, no. 4, pp. 367–380, Mar. 2006.
- [9] M. Colombo, "Experimental investigation and numerical simulation of the two phase flow in the helical coil steam generator," Politecnico di Milano, Milano, Italia, Tesis doctoral, 2013.
- [10] H. Ju, Z. Huang, Y. Xu, B. Duan, and Y. Yu, "Hydraulic Performance of Small Bending Radius Helical Coil-Pipe," Journal of Nuclear Science and Technology, vol. 38, no. 10, pp. 826–831, Oct. 2001.
- [11] J. Liu, M. Masataka, M. Kenichiro, and K. Kazuo, "Pressure drop in two-phase flow through helical coils," International Journal of Heat and Mass Transfer, vol. 44, no. 20, pp. 3993–4003, 2001.
- [12] R. A. Seban and E. F. McLaughlin, "Heat transfer in tube coils with laminar and turbulent flow," International Journal of Heat and Mass Transfer, vol. 6, no. 5, pp. 387–395, May 1963.

- [13] L. Guo, Z. Feng, and X. Chen, "An experimental investigation of the frictional pressure drop of steam water two-phase fow in helical coils," Int. J. Heat Mass Transfer, vol. 44, pp 460-473, 2015.
- [14] X. Zheng et al., "Experimental study on friction pressure drop and circumferential heat transfer characteristics in helical tubes," Front. Energy Res., vol. 11, p. 1204850, June 2023.
- [15] B. K. Hardik, P. K. Baburajan, and S. V. Prabhu, "Local heat transfer coefficient in helical coils with single phase flow," International Journal of Heat and Mass Transfer, vol. 89, pp. 522–538, Oct. 2015.
- [16] L. Santini, A. Cioncolini, C. Lombardi, and M. Ricotti, "Two-phase pressure drops in a helically coiled steam generator," International Journal of Heat and Mass Transfer, vol. 51, no. 19–20, pp. 4926–4939, Sept. 2008.
- [17] Y. Xiao, Z. Hu, S. Chen, and H. Gu, "Experimental study of two-phase frictional pressure drop of steam-water in helically coiled tubes with small coil diameters at high pressure," Applied Thermal Engineering, vol. 132, pp. 18–29, Mar. 2018.
- [18] Y. Su, X. Li, and X. Wu, "Frictional pressure drop correlation of steam-water two-phase flow in helically coiled tubes," Annals of Nuclear Energy, vol. 208, p. 110764, Dec. 2024.
- [19] J.J. Jeong, T.G. Lee, S.G. Nam, and B. Yun, "Incorporating the Effect of Centrifugal Force into the Correlation for Saturated Flow Boiling Heat Transfer in a Helically Coiled Tube," Nuclear Technology, vol. 211, no. 8, pp. 1875–1882, Aug. 2025.
- [20] M. Ciofalo, A. Arini, and M. D. Liberto, "On the influence of gravitational and centrifugal buoyancy on laminar flow and heat transfer in curved pipes and coils," International Journal of Heat and Mass Transfer, vol. 82, pp. 123–134, 2015.
- [21] A. G. Asuero, A. Sayago, and A. G. González, "The Correlation Coefficient: An Overview," Critical Reviews in Analytical Chemistry, vol. 36, no. 1, pp. 41–59, Jan. 2006.
- [22] N. Shrestha, "Detecting Multicollinearity in Regression Analysis," AJAMS, vol. 8, no. 2, pp. 39–42, June 2020.
- [23] T. L. Bergman, D. P. DeWitt, F. Incropera, and A. S. Lavine, Fundamentals of Heat and Mass Transfer, vol. 997. John Wiley & Sons, 2011.
- [24] W. McAdams, W. Woods, and L. Heroman Jr, "Vaporization inside horizontal tubes—II benzene-oil mixtures," Transactions of the American Society of Mechanical Engineers, vol. 64, no. 3, pp. 193–199, 1942.
- [25] S. M. Ghiaasiaan, Two-Phase Flow, Boiling, and Condensation: In Conventional and Miniature Systems, 2nd ed. Cambridge University Press, 2017.
- [26] C. White, Streamline flow through curved pipes, Proc. R. Soc. Lond. Ser. Contain. Pap. Math. Phys. Character 123 (1929) 645–663.
- [27] H. Ito, Flow in Curved Pipes, JSME Int. J. 30 (1987) 543–552. https://doi.org/10.1299/jsme1987.30.543.
- [28] Y. Mori, W. Nakayama, Study on Forced Convective Heat Transfer in Curved Pipes, (2<sup>nd</sup> report, turbulent region), Int. J. Heat Mass Transfer 10 (1967) 37-59.
- [29] E.F. Schmidt, Wärmeübergang und Druckverlust in Rohrschlangen, Chem. Ing. Tech. 39 (1967) 781–789.
- [30] P. Mishra, S.N. Gupta, Momentum Transfer in Curved Pipes. 1. Newtonian Fluids, Ind. Eng. Chem. Process Des. Dev. 18 (1979) 130–137.
- [31] R. Lockhart, R. Martinelli, Proposed correlation of data for isothermal two-phase, two-component flow in pipes, Chem. Eng. Prog. 45 (1949) 39–48. [32] H. Ito, "Flow in Curved Pipes," JSME international journal, vol. 30, no. 262, pp. 543–552, 1987.

- [32] A. Ruffell, Application of homogeneous two-phase friction factor to boiling flow pressure loss calculations, J. Br. Nucl. Energy Soc. 13 (1974) 173–180.
- [33] L. Friedel, Improved friction pressure drop correlations for horizontal and vertical two-phase pipe flow, Eur. Two-Phase Flow Group Meet. Pap. 2 (1979) 1–17.
- [34] L. Zhao, L. Guo, B. Bai, Y. Hou, X. Zhang, Convective boiling heat transfer and two-phase flow characteristics inside a small horizontal helically coiled tubing once-through steam generator, Int. J. Heat Mass Transf. 46 (2003) 4779–4788.
- [35] L. Santini, A. Cioncolini, C. Lombardi, M. Ricotti, Two-phase pressure drops in a helically coiled steam generator, Int. J. Heat Mass Transf. 51 (2008) 4926–4939.
- [36] D.L. Ferraris, C.P. Marcel, Two-phase flow frictional pressure drop prediction in helical coiled tubes, Int. J. Heat Mass Transf. 162 (2020) 120372.
- [37] Y. Su, X. Li, X. Wu, Frictional pressure drop correlation of steam-water two-phase flow in helically coiled tubes, Ann. Nucl. Energy 208 (2024) 110764.